Applications of Ground Penetrating Radar to Hydrogeological Investigations in Coastal Environments

S. Kruse[1], M. Grasmueck[2], L. Bentley[3], S. Guha[1] and T. Juster[1]

1. Dept. of Geology, Univ. of South Florida, 2. Marine Geology and Geophysics, RSMAS, Univ. of Miami, 3. Dept. of Geology and Geophysics, Univ. of Calgary, Canada

ABSTRACT

Ground penetrating radar is sensitive to the porosity and compositional variations common in coastal sands, and hence has become a staple tool for coastal stratigraphers. Under the right circumstances, GPR can also provide very useful information on surficial aquifer hydrogeology in coastal zones. Here we present examples of the primary uses for GPR in coastal hydrogeology: (1) to identify depth to the water table; (2) to estimate the depth to the freshwater/saltwater interface; (3) to map hydrostratigraphic units; and (4) to track water flow and changes in water content in surficial aquifers. The water table generally produces a distinct GPR reflection where the capillary zone is thin relative to the radar wavelength. Uncertainties in the water table depth come primarily from uncertainties in the wave velocity and in the thickness of the capillary fringe. The freshwater/saltwater interface is typically too gradational to reflect energy; instead the radar pulse is attenuated. For some GPR instruments, a very shallow freshwater/saltwater interface can cause saturation in pre-amplifiers, resulting in a spurious high-frequency pulse in the record. On a coastal barrier island in the Outer Banks of North Carolina, GPR proved an excellent tool for mapping a muddy marsh layer that serves as a (semi) confining unit for a perched water table. In siliciclastic and carbonate units in Florida, repeated GPR surveying of individual sites has been used for qualitative tracking of unsaturated zone flow, water table migration, and changes in water content.

1 The Water Table

1A. Resolution of Water Table Depth

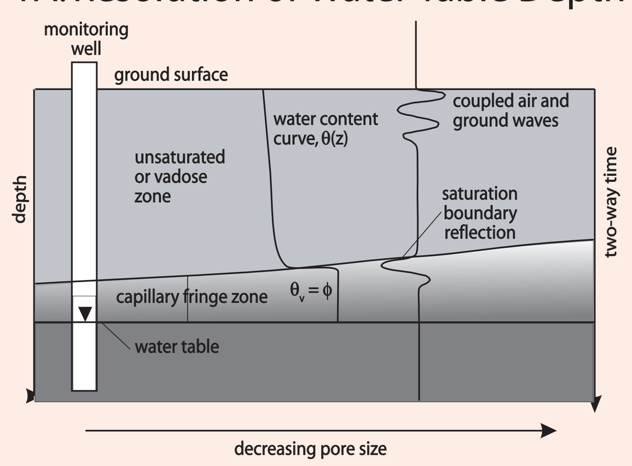

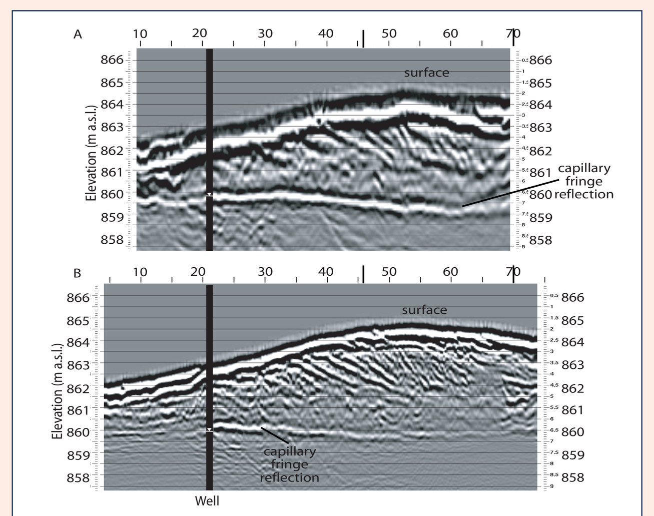

Vertical lines on horizontal axes show CMP locations. Top: 100 MHz. Bottom: 200 MHz. Consistent rise in capillary fringe to left side is interpreted as due to sediment texture changes. From Bentley and Trenholm (2002).

GPR reflections originate from the rapid change in moisture content at the top of the capillary fringe. Bentley and Trenholm (2002) show from study in sand and gravel (although not coastal sands, rather in a quarry near Red Deer, Alberta) that uncertainties in shallow water table depth estimates are on the order of 0.20 m under favorable circumstances. At their test site uncertainties were estimated as shown at right.

Capillary Fringe Depth Uncertainty	
Uncertainty in event pick	+/-0.09m (100 MHz) +/-0.04m (200 MHz)
Velocity uncertainty of a CMP analysis	+/-0.05-0.15m
Velocity uncertainty due to interpolation between CMPs	potentially very large
Uncertainty in event pick due to interference between capillary fringe and other reflectors	potentially very large
Capillary Fringe Height Uncertainty	
Local heterogeneities	+/-0.12m

From Bentley and Trenholm (2002).

When the capillary fringe zone is thicker than the radar wavelength, little energy is reflected. In our experience in coastal sands, the capillary fringe zone is typically prominent at 100 MHz, but this is not true at frequencies higher than 200 MHz. For example, the water table is not readily apparent in the 250 MHz shore-perpendicular survey from Santa Rosa Island, Florida panhandle, shown to the right. At the time of this survey the water table lay at ~0 meter elevation. Gulf of Mexico to left, bay to right.

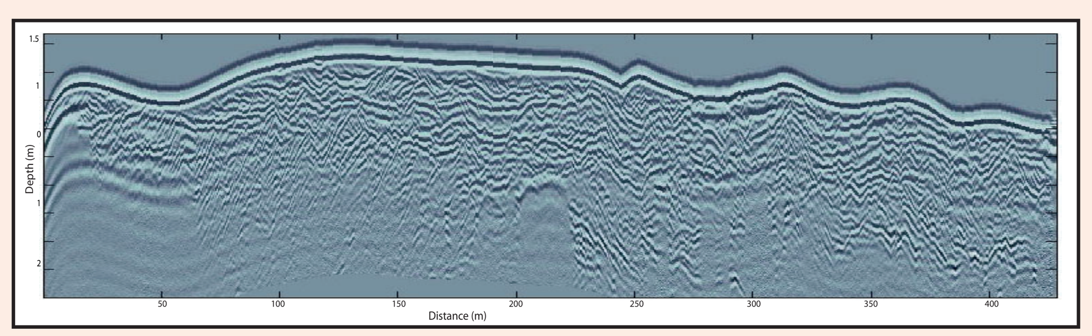

1B. Resolving the Water Table in the Presence of Laminae

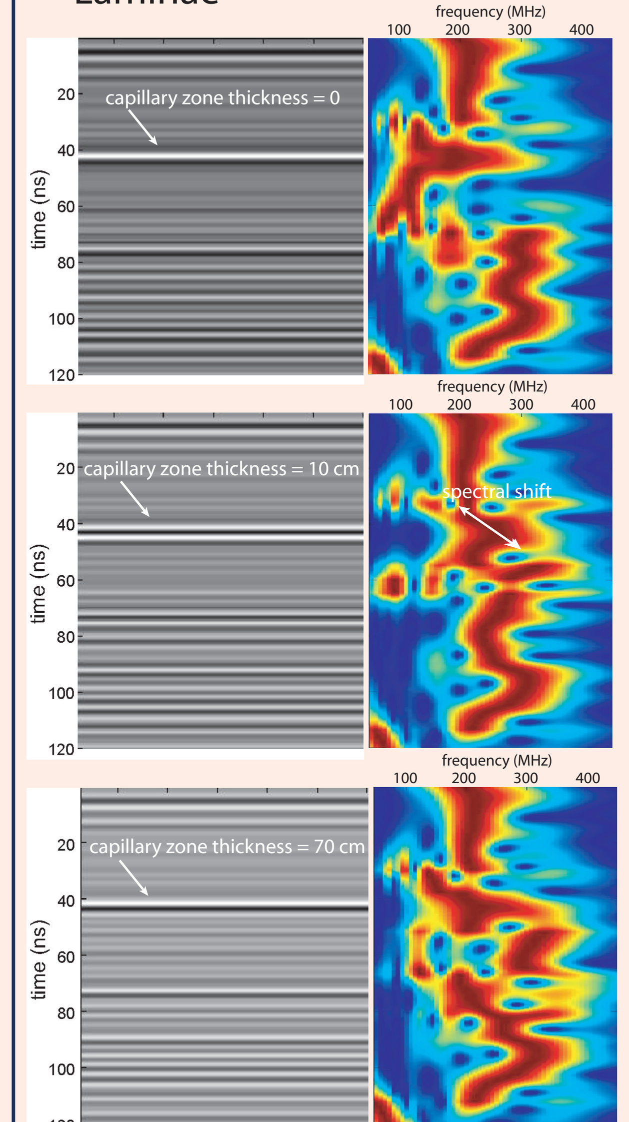

Interpretation of water table reflection is often complicated by interference between the water table return and the response to surrounding thin layers. The figures here show 1D simulations of a 200 MHz GPR response to a "laminated sand" medium with a water table. In the models the top of the capillary fringe is clearly detectable at 40 ns, but the form of the reflection depends on the thickness of the capillary fringe and the local laminations. The models assume a layered sequence with 1mm thick "heavy mineral rich" laminae separated by sand layers with a Gaussian thickness distribution with mean 5mm and std dev 2.5 mm. Model parameters are shown in the box below.

In thin-bedded units one would expect a spectral shift at the water table, as the effective wavelength of the radar wave is shorter in the saturated zone, and higher frequencies will be selectively reflected in the "interference pattern" return. Time-frequency analysis of the 1D model traces shows this effect. Here, the time-frequency diagrams (shown to right of model radar profiles) have been done using the S-Transform, a Gaussian window function that translates along the length of each trace, with window length determined by the frequency content.

model parameters		εr	μr	σ	thickness
unsaturated zone	Layer 1	24	1.2	0.004 S/m	1 mm
	Layer 2	4	1.0	0.001 S/m	5+/-2.5 mm
saturated zone	Layer 1	38	1.2	0.004 S/m	1 mm
	Layer 2	20	1.0	0.001 S/m	5+/-2.5 mm

1C. Using the Water Table as a Horizontal Reference Surface

On small low barrier islands the water table is close enough to horizontal (elevations <~ 1m) that we have used it as a reference horizon for plotting GPR profiles where topography was poorly known or could not be measured with GPS due to canopy. An example is shown below for a shore-parallel traverse along the central part of North Island, South Carolina.

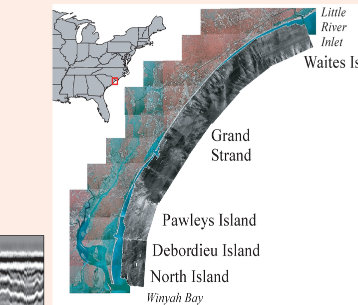

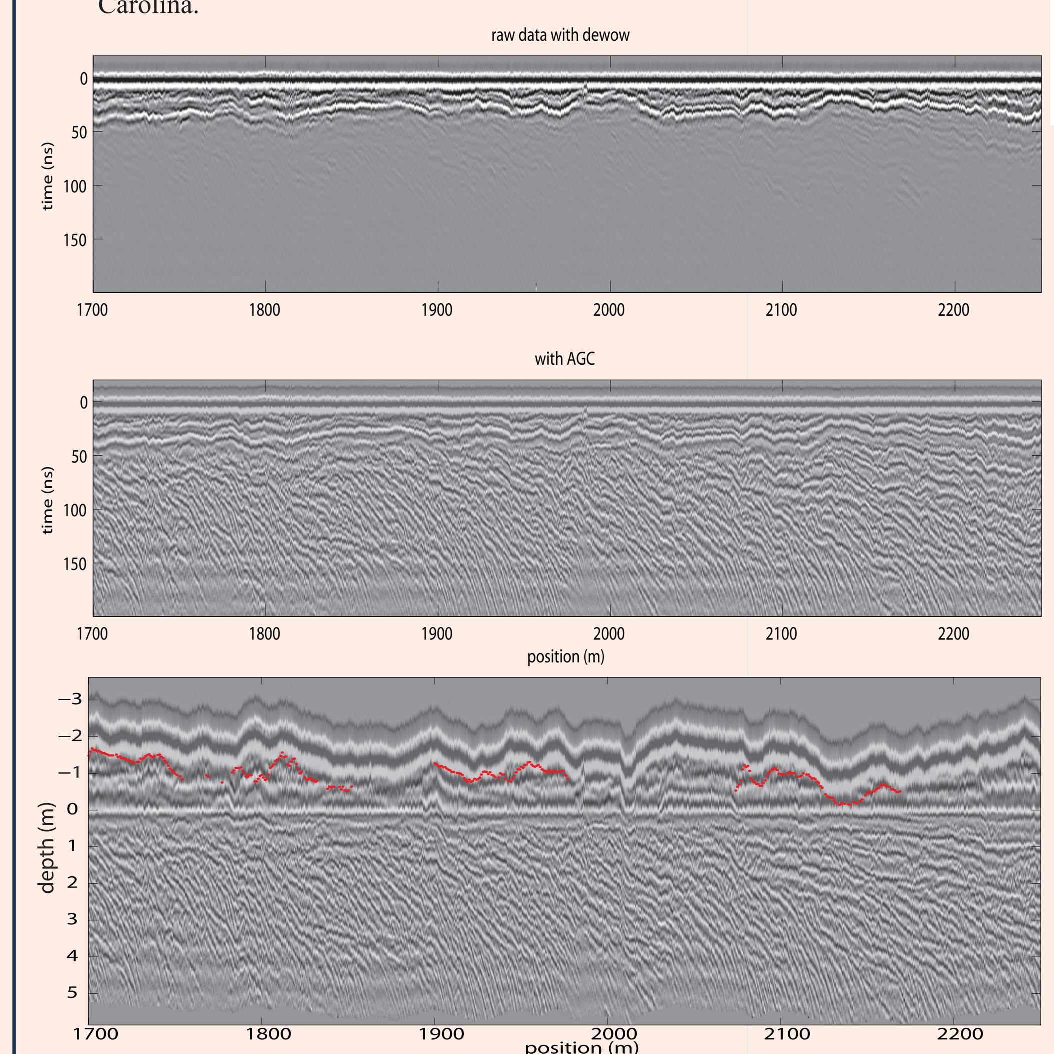

Top: Raw 100 MHz data, only dewow filter applied. The water table is the lowermost prominent reflector.

Middle: With AGC gain, 15 ns window, applied.

Bottom: Water table arrival times are picked. Travel times are then converted to depths using CMP-derived velocities of 0.12 m/ns for the unsaturated zone and 0.065 m/ns for the saturated zone. The water table is set to 0 m depth. Red dots show measured elevations, where canopy permitted. Remarkably, the fit between GPR-inferred and observed topography is good to within 0.5 meters, despite the assumption of a uniform velocity throughout the unsaturated zone.

2 The Freshwater/Saltwater Interface

The freshwater/saltwater mixing zone is typically thicker than the radar wavelength, and does not cause a reflection. The signal attenuation associated with high conductivity saline water is clear in some settings (figure to right). In most settings, however attenuation must be interpreted with care. For example, in the figure below the lack of returns from depth around the 350 m location is due to lack of penetration through a marsh mud layer at ~1.5 m depth. Interpretation of freshwater/saltwater interface from GPR records needs to be locally calibrated.

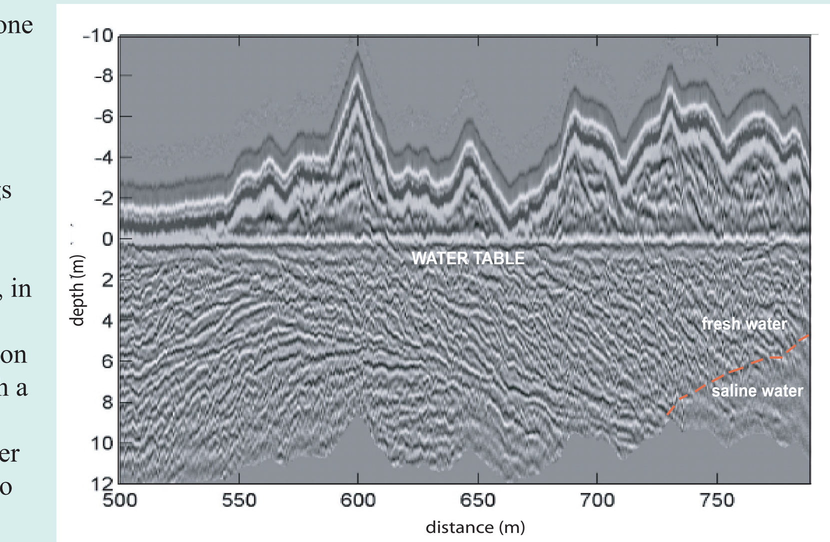

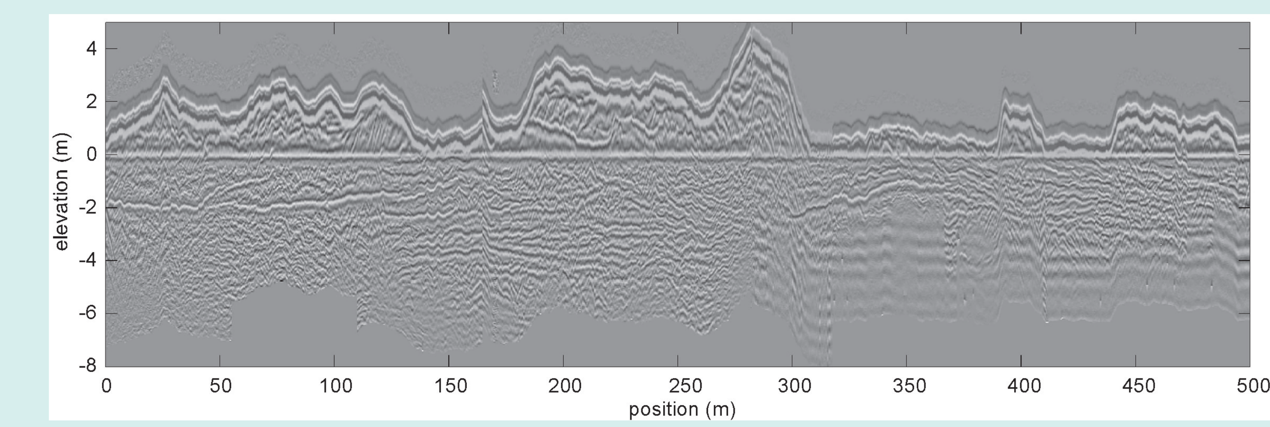

Top: Beach-perpendicular profile across North Island, South Carolina, 100 MHz antennas, AGC gain, 15 ns window. Times converted to depths/elevations assuming unsaturated zone velocity of 0.08 m/ns, saturated zone velocity 0.065 m/ns. Water table is set to 0 elevation. Atlantic ocean is to right, mainland to left.

Bottom: Beach-perpendicular profile across Waites Island, South Carolina, 100 MHz antennas, AGC gain, 15 ns window. Times converted to depths/elevations assuming unsatuated zone velocity of 0.12 m/ns, saturated zone 0.06 m/ns. Water table is set to 0 elevation. Atlantic Ocean to right, mainland to left. Horizonal banding in lower right is instrument noise.

3 Hydrostratigraphic Units

GPR is very sensitive to sand-mud and sand-clay transitions. Mud or clay horizons often function as semiconfining units in surficial coastal aquifers. At the example site shown here, on the Outer Banks near Salvo, North Carolina, a transect of water table elevations across the island indicated a better fit to a perched aquifer model than a unconfined Baden Ghyben-Herzberg lens (see figure below). The water table elevations were best fit by a model with the lens truncated at 3 m depth.

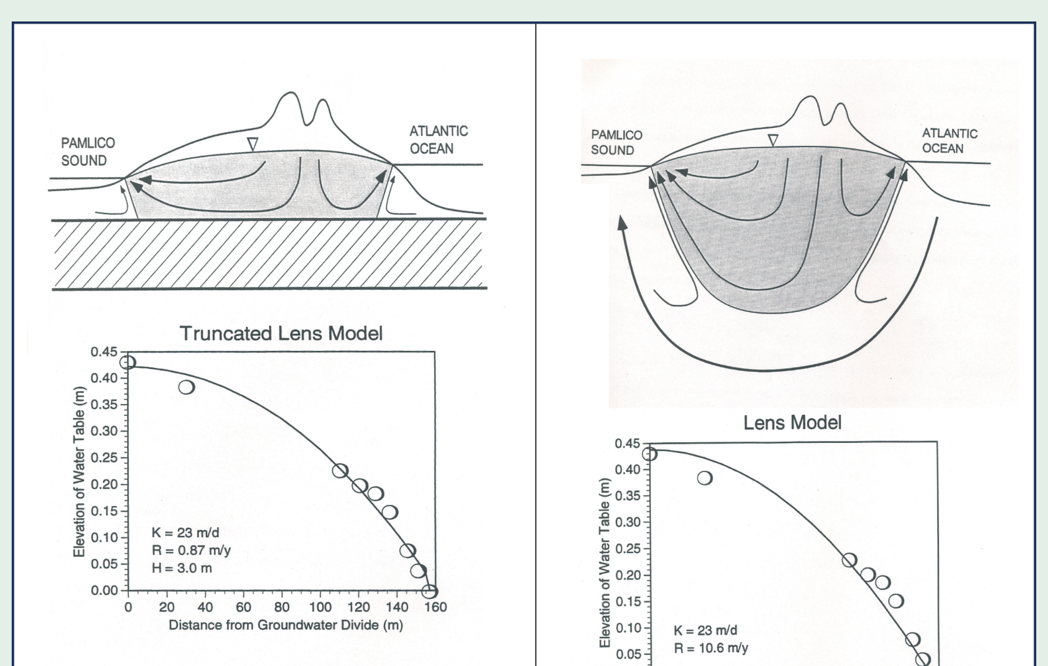

From Nogi, 1996.

A GPR profile run close to the water table transect clearly shows a very bright reflector at about 3 meters depth (figure to right). We interpret this reflector as the response to a mud layer that could be seen in the intertidal zone at very low tide. Signal from below this bright reflector is strongly attenuated. This may be due to lack of energy transmitted through the mud, but may also indicate an abrupt transition from freshwater to more saline water across the confining mud layer.

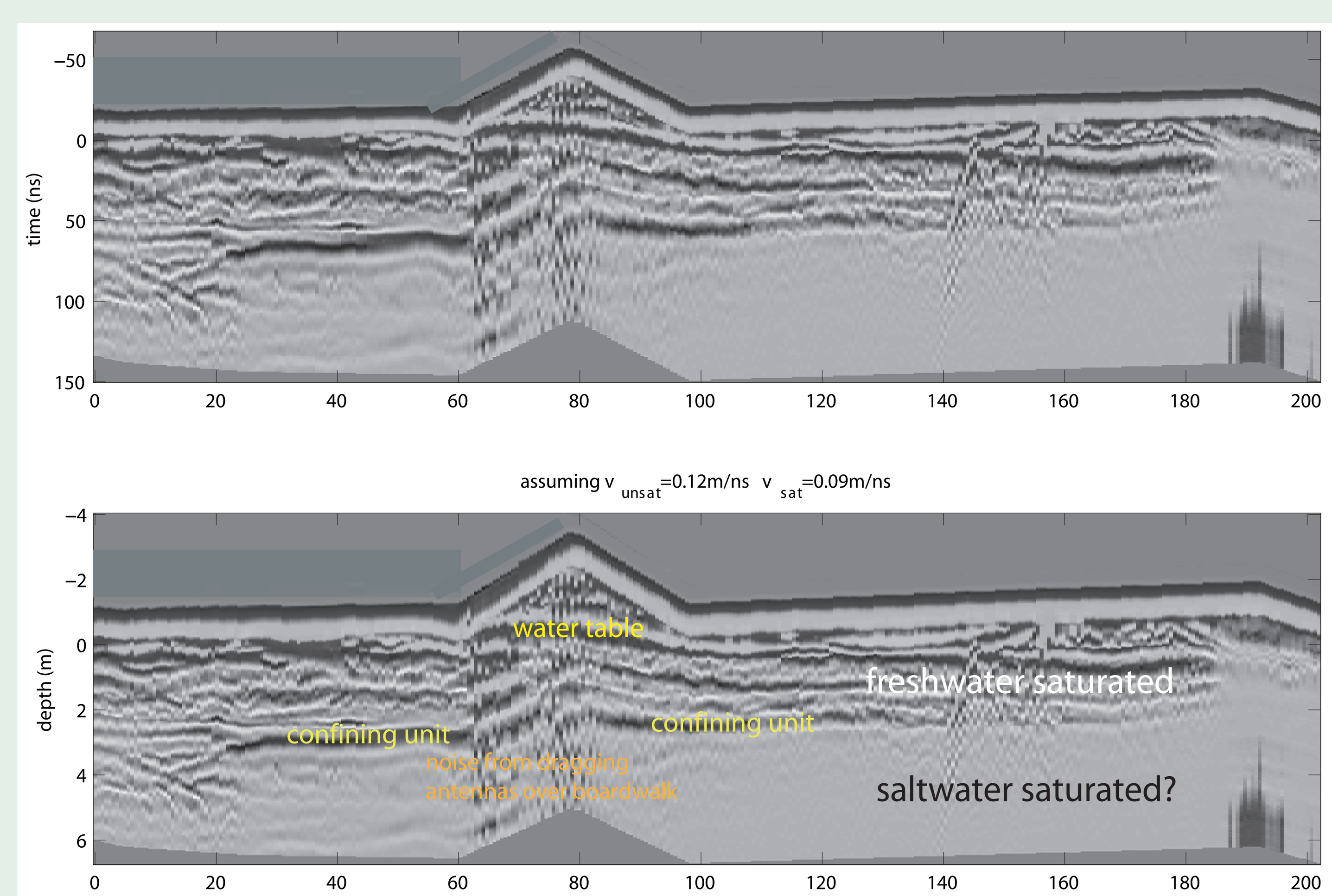

From Werner, 1996.

4 Tracking Unsaturated Zone Flow

Preferential flowpaths in the unsaturated zone can be tracked by repeated imaging with GPR. Local increases in water content are detected through increases in both reflection arrival time and reflection amplitudes. Here, 3D surveys repeated hourly over a small sink in the oolitic Miami Limestone show downward movement of the wetting front within a conduit. Later surveys show lateral migration of the wetting front, with preferential propagation in the direction of the strike of stratigraphic units. From Truss et al., *submitted*.

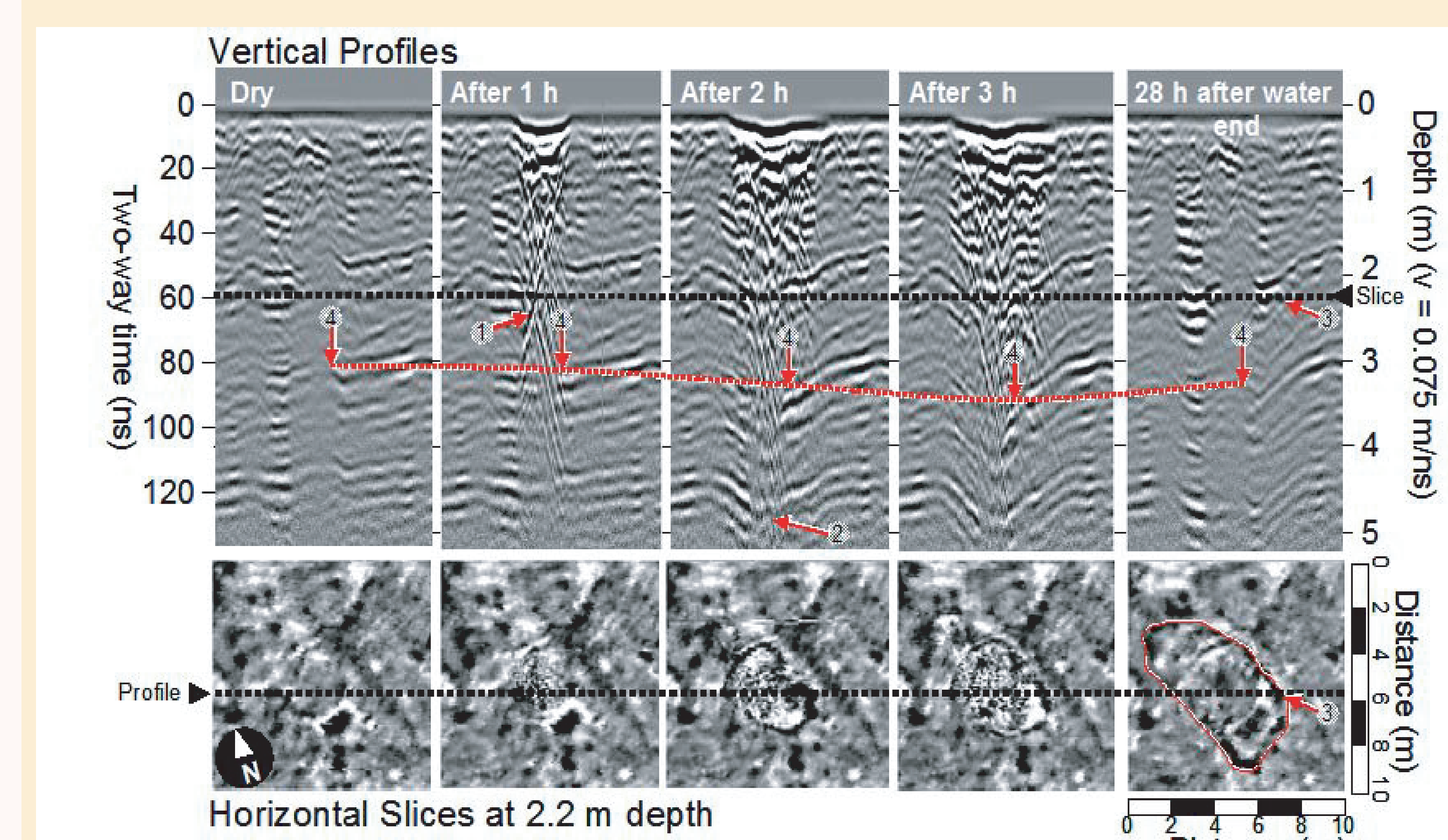

From Truss et al., *submitted*.

Vertical profiles and horizontal slices extracted from the repeated 3D GPR data volumes show effects of moisture movement in the subsurface due to water introduced at the surface of a sink. Ponding of water at the surface causes a delay in the first arrival and increases amplitude level of signals below. Pointers (1) and (2) show vertical progress of the wetting front within the sink of 2.4 m/h. After turning off the water and waiting for 28 h, amplitudes within the sink have returned to pre-injection condition. However, brighter amplitudes are visible outside the sink (event 3). The horizontal slice indicates preferential propagation of the wetting front in NW-SE direction, parallel to the strike of the stratigraphic units. Pointer 4 indicates significant time shifts of up to 10 ns throughout the injection test, starting at dry with reflectors inside the sink appearing to be pulled up similar to hockey sticks indicating relatively dryer conditions in the sink than in the surrounding rock. As the volume of water in the sink increases, the GPR events are delayed, partly returning towards initial start levels by 28 h after injection end.

ACKNOWLEDGEMENTS

Scott Harris, Mark Horwitz, Ulrich Kruse, Jill Nogi, Danya Pace, Nicole Trenholm, Steven Truss, Sandra Vega, David Viggiano, Heidi Werner, and Eric Wright contributed to the projects cited here. These projects were variously funded by the NSERC, University of Calgary Collaborative Research Grant, USGS, South Carolina Sea Grant Consortium, University of Miami Innovative Teaching and Technology Initiative, Comparative Sedimentology Laboratory, ACS Petroleum Research Fund, and NSF.

REFERENCES

Bentley, L.R. and N.M. Trenholm, The accuracy of water table elevation estimates determined from ground penetrating radar data, *J. Env. Eng. Geophys.*, 7(1), 2002.

Guha, S., S.E. Kruse, E.E. Wright, and U.E. Kruse, Spectral analysis of ground penetrating radar response to thin sedimentary layers, *Geophys. Res. Lett.,* 32, L23304, doi:10.1029/2005GL023933 (2005).

Nogi, J., Driving Force(s) for Nearshore Submarine Groundwater Discharge into Pamlico Sound, Hatteras Island, North Carolina, B.S. thesis, College of William and Mary, 1996.

Truss, S., M. Grasmueck, S. Vega, and D. Viggiano, Using high resolution 4D GPR to image preferential flowpaths within the Miami Oolitic Limestone, under revision, *Water Res. Res*.

Werner, H., A Test of the Effectivness of Ground Penetrating Radar in a Barrier Island Setting, B.S. thesis, College of William and Mary, 1996.